Aging Cell (2011) **10,** pp148–157 Doi: 10.1111/j.1474-9726.2010.00654.x

Restoration of senescent human diploid fibroblasts by modulation of the extracellular matrix

Hae Ri Choi[1]*, Kyung A Cho[2]*, Hyun Tae Kang[1], Jung Bin Lee[3], Matt Kaeberlein[4], Yousin Suh[5,6], In Kwon Chung[7] and Sang Chul Park[1]

[1]Department of Biochemistry and Molecular Biology, Aging and Apoptosis Research Center, Institute on Aging, Seoul National University College of Medicine, 28 Yongon-Dong, Chongno-Gu, Seoul 110-799, South Korea
[2]Department of Biochemistry, Chonnam National University Medical School, Gwangju, South Korea
[3]Department of Forensic Medicine, Seoul National University College of Medicine, 28 Yongon-Dong, Chongno-Gu, Seoul 110-799, South Korea
[4]Department of Pathology, University of Washington, Seattle, WA 98195, USA
[5]Institute for Aging Research, Diabetes Research and Training Center and [6]Departments of Medicine and Genetics, Albert Einstein College of Medicine, Bronx, NY, USA
[7]Departments of Biology and Biomedical Sciences, Yonsei University, Seoul, South Korea

Summary

Human diploid fibroblasts have the capacity to complete a finite number of cell divisions before entering a state of replicative senescence characterized by growth arrest, changes in morphology, and altered gene expression. Herein, we report that interaction with extracellular matrix (ECM) from young cells is sufficient to restore aged, senescent cells to an apparently youthful state. The identity of the restored cells as having been derived from senescent cells has been confirmed by a variety of methods, including time lapse live cell imaging and DNA finger print analysis. In addition to cell morphology, phenotypic restoration was assessed by resumption of proliferative potential, growth factor responsiveness, reduction of intracellular reactive oxygen species levels, recovery of mitochondrial membrane potential, and increased telomere length. Mechanistically, we find that both Ku and SIRT1 are induced during restoration and are required for senescent cells to return to a youthful phenotype. These observations demonstrate that human cellular senescence is profoundly influenced by cues from the ECM, and that senescent cell plasticity is much greater than that was previously believed to be the case.

Key words: Aging; cellular senescence; extra cellular matrix; Ku70; SIRT1.

Correspondence
Sang Chul Park, Department of Biochemistry and Molecular Biology, Aging and Apoptosis Research Center, Institute on Aging, Seoul National University College of Medicine, 28 Yongon-Dong, Chongno-Gu, Seoul 110-799, South Korea. Tel.: 82 2 744 4534; fax: 82 2 744 4534; e-mail: scpark@snu.ac.kr

*These authors contributed equally to this work.

Accepted for publication *1 November 2010*

Introduction

The microenvironment in which a cell resides has a profound effect on cellular function and physiology. The nature of this microenvironment is determined in large part by synthesis and secretion of a variety of factors, especially components of the extracellular matrix (ECM). The ECM is a complex, three-dimensional network of macromolecules that provides spatial information and an architectural scaffold for cells. Moreover, the ECM coordinates cell organization within tissues, and supports manifold activities of cells by modulating signal transduction (Hynes, 2009).

Most human cells are capable of only a finite number of cell divisions before arresting growth and entering a nondividing state referred to as replicative senescence. Cell division potential is in general limited by telomere shortening, which occurs gradually with each mitotic division in cells not actively expressing telomerase (Harley *et al.*, 1990). Telomeres provide essential protection for chromosome ends, and when telomere lengths are sufficiently reduced, a DNA damage response (DDR) is initiated that terminally arrests the cell cycle. In rare cases, telomerase-negative cells are able to escape replicative senescence by elongating their telomeres through a telomerase-independent alternative lengthening mechanism referred to as ALT (Henson *et al.*, 2002). In mammals, several of the proteins involved in the nonhomologous end joining (NHEJ) DNA repair pathway are telomere bound and affect telomere length maintenance (Gasser, 2000). These include Ku70 and Ku80, which form a heterodimer (Ku) that can bind to free double-stranded DNA ends. Inactivation of Ku leads to various defects including telomere length deregulation and end-to-end chromosome fusions (Critchlow & Jackson, 1998; Indiviglio & Bertuch, 2009). Sirtuins are Nicotinami de adenine dinucleotide (NAD^+)-dependent class III histone deacetylases that have been linked to the onset of senescence (Longo & Kennedy, 2006). Over expression of SIRT1 orthologs leads to lifespan extension in yeast, flies, and worms (Kaeberlein *et al.*, 1999; Finkel *et al.*, 2009). Yeast Sir proteins perform multiple biological functions, including localizing to sites of DNA double strand breaks (Kennedy *et al.* 1997) and modulating their repair by NHEJ (Tsukamoto *et al.*, 1997; Haber, 1999), although there is some evidence that this finding is at least partially an indirect consequence of derepressing silent mating types loci (Astrom *et al.*, 1999; Lee *et al.*, 1999). The roles of SIRT1 in NHEJ are poorly understood in mammals;

Aging Cell

however, there is evidence that SIRT1 influences DNA repair (Wang *et al.*, 2008) at least in part by promoting the deacetylation of Ku70 (Cohen *et al.*, 2004; Jeong *et al.*, 2007).

The degree to which replicative senescence contributes to aging remains unknown; however, it is clear that telomere length shortens *in vivo* in a variety of cells types, and senescent cells accumulate during human aging (Cawthon *et al.*, 2003; Canela *et al.*, 2007). It has been speculated that this accumulation of senescent cells plays an important role in age-associated declines in tissue function and the progression of age-related diseases. Consistent with this idea, telomere length has been found to correlate inversely with donor age in multiple cell types, and has been reported to be predictive for survival in a few cases (Herbig *et al.*, 2006; Jeyapalan & Sedivy, 2008). Although a causal role for telomere shortening as a significant molecular cause of aging has yet to be established (Gorbunova & Seluanov, 2009) and may be species specific (Wright & Shay, 2000; Lund *et al.*, 2009). Somatic cells lacking telomerase gradually lose telomeric sequences as a result of incomplete replication (Harley *et al.*, 1990; Hastie *et al.*, 1990) and eventually progress into senescence (Allsopp *et al.*, 1992).

The age-related senescent phenotype is in general regarded as absolute and irreversible (Pereira-Smith & Smith, 1981; Linnane *et al.*, 1989; d'Adda di Fagagna, 2008). Cell hybridization studies have demonstrated that senescence is dominant over the young phenotype or even tumor phenotype (Muggleton-Harris & DeSimone, 1980; Krtolica *et al.*, 2001), and there is currently no known method for restoring aged, senescent cells to the young state. However, recent discoveries have suggested that the tissue microenvironment has a remarkable capability to alter cellular fate and even rejuvenate aspects of age progenitor cells (Conboy, Conboy *et al.*, 2005). Herein, we furthermore define the importance of microenvironment during cellular aging with the striking observation that ECM from young cells is sufficient to restore multiple features of the youthful phenotype in senescent diploid human fibroblasts. This restoration includes the ability to resume apparently normal proliferation for approximately 25 additional population doublings, corresponding to a 39% increase in cellular lifespan.

Results

Young ECM restores proliferative capacity of senescent cells

To test whether the senescent phenotype of diploid fibroblasts is influenced by microenvironment, we isolated ECM from young cells (Y-ECM) and plated senescent cells onto either Y-ECM or onto ECM from old senescent cells (O-ECM). In parallel, we also plated young cells onto either Y-ECM or O-ECM and monitored growth and morphology. As expected, young cells were able to continue growth and maintain normal morphology on either ECM (Fig. 1A). Interestingly, there was a noticeable delay in outgrowth of young cells plated onto O-ECM relative to cells on Y-ECM (Fig. 1B), suggesting that the old ECM is not optimal for growth of young cells. Also as expected, senescent cells plated on O-ECM remained senescent and showed no obvious changes in morphology (Fig. 1C). In contrast, senescent cells plated on the Y-ECM showed morphological changes consistent with restoration of the youthful state. These changes occurred over the first few days after plating onto Y-ECM and, within 1 week, the formerly senescent cells had resumed proliferation and were morphologically indistinguishable from young cells (Fig. 1C,D). Restoration of division potential in formerly senescent cells by Y-ECM was verified by time lapse live cell analysis (Fig. S1). The normally flat and enlarged morphology of senescent cells on Y-ECM gradually changed into spindle-like shapes, followed by the formation of two small daughter cells. To rule out the possibility that the restored cells were derived from a small number of original young cells remaining in the young cell derived matrix preparations, we prepared Y-ECM from neonatal fibroblasts, a different source of cells, and assessed their ability for restoration of senescent cells compared with cells of a 6-year-old boy (Fig. S3A). The ECM from the neonatal cells had exactly the same effect as the Y-ECM derived from young cells (6-year-old boy) (Fig. S3B). In addition, DNA fingerprinting analysis confirmed the origin of the restored cells as being from the senescent cells (Fig. S3C), demonstrating the genuine effects of ECM derived from young vs. senescent cells and its ability to restore growth and morphological changes of senescent cells. This finding was independently confirmed by following the conversion of red fluorescent protein (RFP)-tagged senescent cells on Y-ECM during restoration, into youthful appearing spindle shaped cells (Fig. S2).

Restored senescent cells display multiple characteristics of young cells

To furthermore characterize the phenotypic reversion of senescent cells induced by Y-ECM, we monitored several defined markers of cellular senescence. Relative to senescent cells on O-ECM, the restored senescent cells showed lower SA-β-gal activity (Dimri *et al.*, 1995) and reduced intracellular reactive oxygen species (ROS) levels (Harman, 1956) that were comparable to young cells (Fig. 2A**,** second, and third panel)**.**The F-actin staining of restored cells also revealed morphologic and intracellular actin structure patterns similar to those of young cells (Fig. 2A, first panel). Consistent with their ability to resume cell proliferation, DNA synthesis was observed in restored senescent cells by BrdU incorporation (Fig. 2B). Comparison of mitochondrial membrane potentials ($\Delta\Psi_m$) in young, senescent, and restored-senescent cells also suggested that mitochondrial function was improved in the restored cells, as evidenced by suppression of the reduced $\triangle\Psi_m$ of senescent cells (Fig. 2E). We have previously reported that senescent cells are resistant to both apoptotic signals (Ryu *et al.*, 2007) and epidermal growth factor (EGF) stimulation (Park *et al.*, 2000). Restored senescent cells showed active extracellular signal-regulated kinase (ERK) phosphorylation in response to EGF (Fig. 2D) (Wang & Walsh, 1996) and a concomitant reduction of cell cycle inhibitory molecules

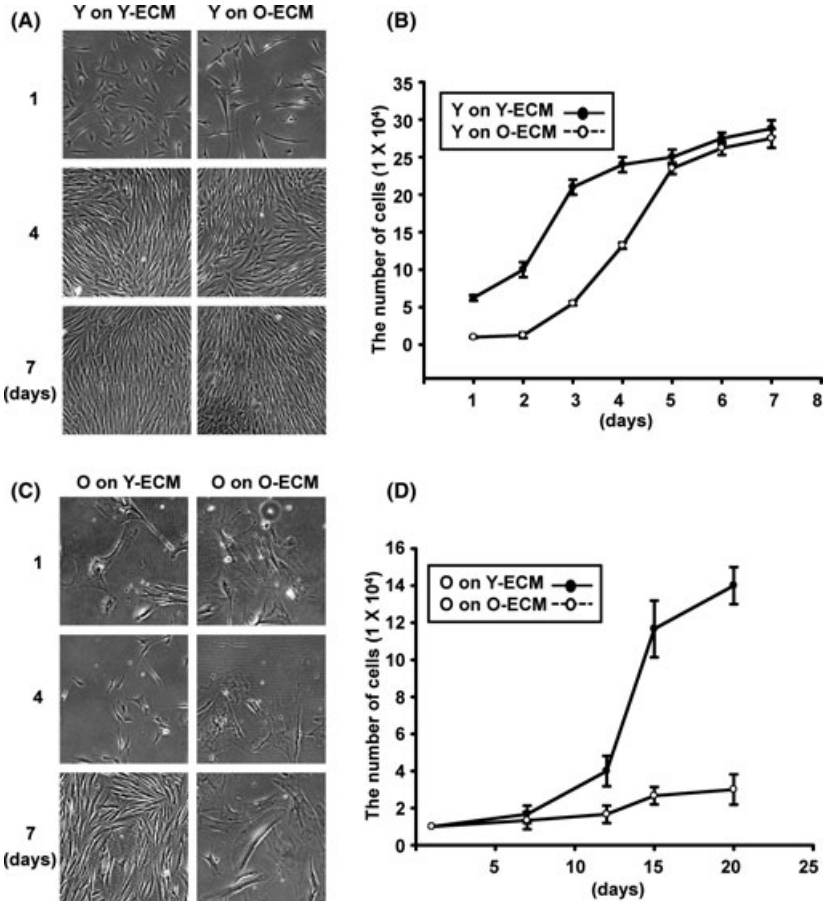

Fig. 1 Young extracellular matrix (ECM) restores proliferative capacity of senescent cells (A) Young cells (Y) on ECM derived from young or senescent cells (Y-ECM or O-ECM, respectively,) were analyzed under light microscope for indicated time. (B) Comparison of total cell counts in young cells on Y-ECM or O-ECM. (C, D) Morphology and proliferation data for senescent cells (O) analyzed using the same methods.

(Deng *et al.*, 2008), such as $p21^{Waf1}$, $p16^{INK4a}$, p53 and caveolin-1 (Fig. 2C), indicating restored growth factor responsiveness and robust cell cycle progression.

To exclude the possibility that the mitogenic activity of the restored senescent cells might be associated with transformation of senescent cells during restoration process, we carried out soft agar colony assays. In contrast to HeLa cancer cells, which form colonies readily in soft agar, the restored senescent cells were not able to form any colonies (Fig. 2H).

As furthermore support for the idea that restored senescent cells are not transformed, proliferation of restored cells was arrested after approximately 25 population doublings (Fig. 2G), at which point they reverted to an apparently normal senescent state with the typical characteristics of decreased growth; flattened and enlarged cell shapes; and high SA-β-gal activity (Fig. 2F).

Restored senescent cells show elongated telomeres

Replicative senescence of fibroblasts in culture occurs as a result of telomere shortening. When telomeres become terminally short, they are recognized by DNA repair machinery as a DNA double strand break, leading to induction of a persistent DDR (Gasser, 2000; Verdun & Karlseder, 2007). Using the highly sensitive comet assay (Olive & Banath, 2006), we were able to observe a high level of DNA breaks in individual senescent cells (Fig. 3A)**.** This damage was undetectable in restored senescent cells or young cells (d'Adda di Fagagna *et al.*, 2003). A similar trend was observed using immuno-fluorescence analysis of DDR and dysfunctional telomere-induced foci (Takai *et al.*, 2003). A marker of the DDR, gamma-H2AX foci was detectable in senescent cells. Thirty-six percent of gamma-H2AX foci were co-localized with dysfunctional telomeres to form dysfunctional telomere-induced foci. However, these foci were rarely observed in restored senescent or young cells (Fig. 3B). These data suggest that telomere ends are no longer being recognized as DNA double strand breaks in restored senescent cells. The absence of detectable DNA damage in restored senescent cells along with their resumption of apparently normal proliferation suggested one of two possibilities. Either telomeres remained short and the signal for DNA damage was being bypassed, or telomere length was being restored. To differentiate between these possibilities, we determined whether telomere elongation had occurred in restored senescent cells on Y-ECM. Relative to senescent cells, restored senescent cells on Y-ECM showed elongated telomeres approaching, but not quite reaching, the length of young cells (Fig. 3C).

Telomerase acts as a reverse transcriptase that synthesizes the G-rich strand of telomeric DNA to compensate for the shortening observed with the DNA end replication problem (Blackburn,

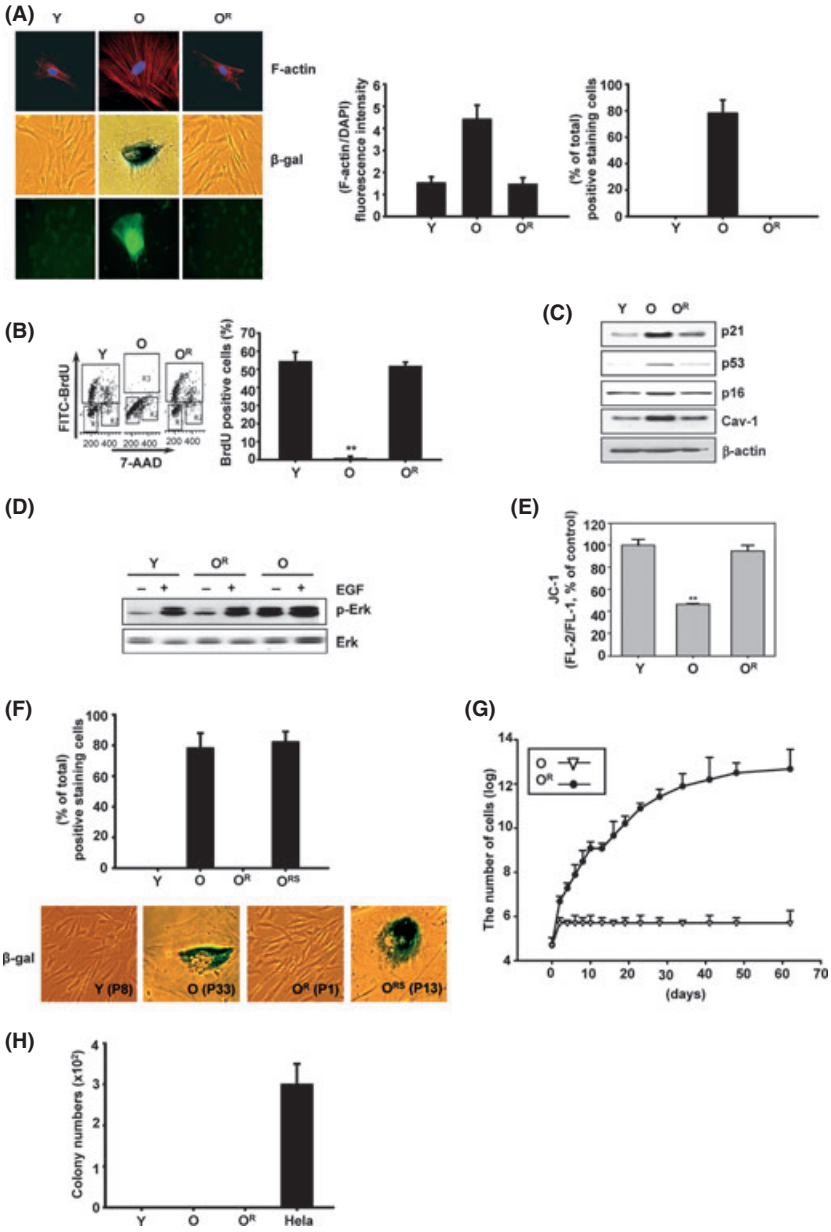

Fig. 2 Restored senescent cells display multiple characteristics of young cells (A) Young (Y), senescent (O) or restored senescent (O^R) cells represented SA-β-gal activity (second panel), cellular ROS levels (third panel), analyzed by CM-H_2DCF-DA and morphological changes (first panel), analyzed by staining of F-actin (red) and DAPI (blue). (B) The levels of cellular BrdU incorporation in young, senescent, and restored senescent cells, indicating active DNA synthesis. (R3-BrdU positive cells) (C) Expression levels of p21, p53, p16 and caveolin-1 in young, senescent or restored senescent cells were analyzed by Western blotting. (D) Total lysates from young, senescent, and restored senescent cells (treated with EGF at 100 ng mL^{-1} for 30 min) analyzed by Western blotting using polyclonal anti-phospho-Erk antibody. (E) Mitochondrial membrane potential in young, senescent or restored senescent cells. A double asterisk (**) denotes the statistical significance between young vs. senescent cells, $P < 0.001$; and between senescent vs. restored senescent cells, $P < 0.001$ in a student's *t* test. (F) Young (passage 8), senescent (passage 33), restored senescent (passage 1) and re-senescent (O^{RS}, passage 12) cells were incubated with SA-β-gal staining solution. (G) Growth curve of restored senescent cells or senescent cells. (H) HeLa, young, senescent or restored senescent cells were individually suspending in 10% FBS and 0.3% top agar seeded on to 0.6% base agar in 60 mm Φ plates. After 3 weeks, the cells were stained with Trypan Blue and the number of colonies was counted under the microscope. Histograms indicate the mean and the error bars indicate the standard deviation of the mean.

1990). To examine whether the recovered telomere length in restored senescent cells is by telomerase re-activation, we measured telomerase activity by telomeric repeat amplification protocol (TRAP) assay and RT-PCR. Interestingly, we were unable to detect telomerase activity during the restoration process (Fig. 3D); raising the possibility that telomere elongation occurs during the restoration process via a telomerase-independent mechanism.

Ku is required for restoration of senescent cells

Given the absence of detectable telomerase activation, we explored the involvement of the telomere-related Ku DNA repair pathway, since the DNA damage of senescent cells is no longer apparent in restored senescent cells. During normal senescence, Ku protein declines in abundance relative to young cells**.** However, this decrease in Ku expression was reversed during Y-ECM restoration, with Ku levels gradually increasing during the restoration process (Fig. 4A). When Ku70 was down-regulated by siRNA, the expression level of both Ku70 and Ku80 was decreased (Fig. S4A).

To determine whether Ku plays a role in restoration, we examined whether knockdown of Ku70 influenced the ability of Y-ECM to restore senescent cells. Ku70-deficient cells are known to have defects in telomere end capping and DNA damage signaling (Fig. S4B,C), which results in genomic instability and accelerated cellular senescence (Fisher & Zakian, 2005; Seluanov *et al.*, 2007). Remarkably, knock-down of Ku70 resulted in a loss of the ability of Y-ECM to induce restoration of senescent cells (Fig. 4B,C).

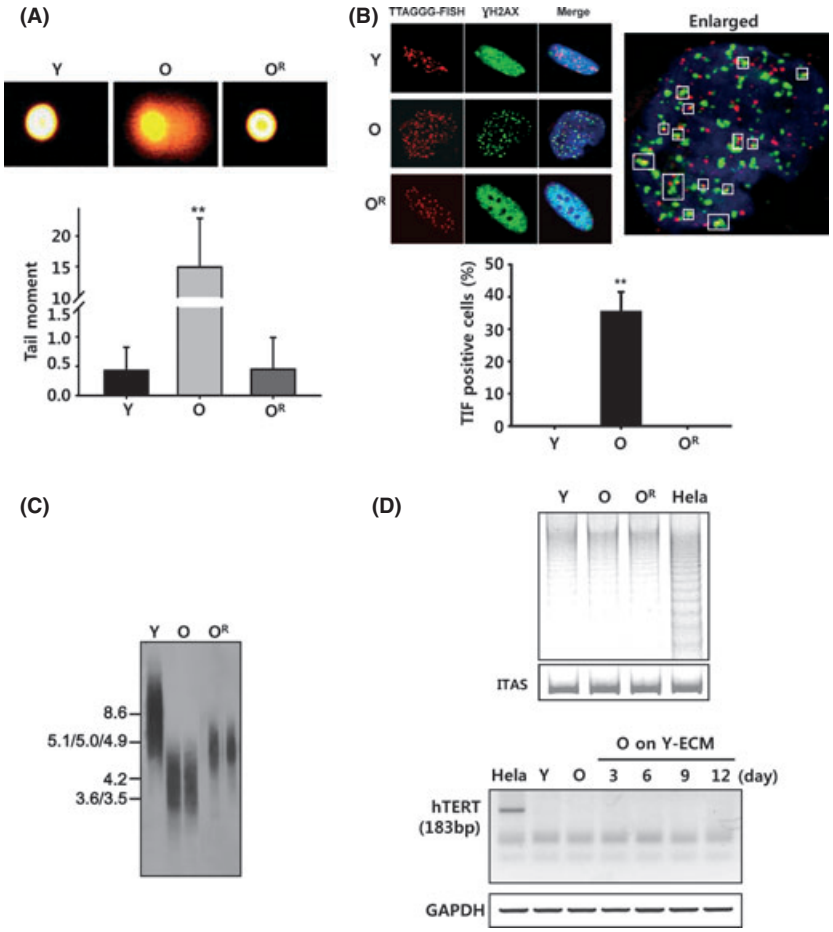

Fig. 3 Restored senescent cells show elongated telomeres (A) Comet assay was carried out for detection of DNA damage among young, senescent, and restored senescent cells. The DNA 'comet' tail shape and migration pattern of young, senescent and restored senescent cells were analyzed under UV- microscope. Histogram indicates average evaluation of the DNA 'comet' tail in young, senescent, and restored senescent cells. A double asterisk (**) denotes the statistical significance between young vs. senescent cells, $P < 0.001$; and between senescent vs. restored senescent cells, $P < 0.001$ in a student's t test. ($n = 70$) (B) Accumulation of gamma-H2AX on uncapped telomeres. Young, senescent, and restored cells were processed for immunofluorescence using gamma-H2AX (green), DAPI (blue) and Telomeric DNA (red). Histogram indicates telomere-dysfunction-induced foci (TIF) index (percentage of dysfunctional telomere-induced foci positive cells). Young, senescent, and restored cells with gamma-H2AX foci co-localizing with telomeric DNA were scored as TIF positive. A double asterisk (**) denotes the statistical significance between young vs. senescent cells, $P < 0.001$; and between senescent vs. restored senescent cells, $P < 0.001$ in a student's t test. ($n = 50$ from two independent experiments) (C) Telomere length was analyzed by Southern blotting. (D) Telomerase activity was monitored by the telomeric repeat amplification protocol assay and RT-PCR during the restoration process.

SIRT1 is required for Ku-dependent restoration

The NAD-dependent protein deacetylase SIRT1 is required for efficient DNA double strand break repair (Hasty, 2001; Vijg *et al.*, 2008). It plays an important role in genomic stability and is able to deacetylate and activate Ku70 (Haber, 1999; Cohen *et al.*, 2004; Jeong *et al.*, 2007; Oberdoerffer *et al.*, 2008). Similar to the changes in Ku abundance, SIRT1 abundance also decreased during normal senescence, but was increased again during the restoration process (Fig. 5A). Ku70 acetylation state correlated inversely with SIRT1 abundance (Fig. S5), consistent with observed changes in SIRT1 protein levels and suggesting the possibility that these changes may be related to the ability of Y-ECM to restore old senescent cells. To test this possibility, we cultured senescent cells on Y-ECM in the presence of 1 μM EX-527, a specific and potent inhibitor of SIRT1 activity. Treatment with EX-527 caused an increase in the acetylation of Ku70 in young cells and completely suppressed the ability of Y-ECM to induce restoration of senescent cells (Fig. 5C,D).

Discussion

Cells influence their microenvironment through synthesis and secretion of a variety of factors including the components of the ECM. Soluble and insoluble factors secreted by senescent cells have been shown to contribute to cancer progression in aged organisms and to influence epithelial cell growth and tumorigenesis, suggesting an active role for ECM in determining cellular fate (Krtolica *et al.*, 2001; Campisi & d'Adda di Fagagna, 2007). In this study, we have shown that ECM from young cells is sufficient to overcome the senescence barrier (Fig. 1C,D) of human fibroblasts without transformation (Fig. 2H), providing approximately 25 additional population doublings (PDs) of apparently normal replicative potential (Fig. 2F,G). These results clearly illustrate that important differences exist between ECMs of young and senescent cells, and that maintenance of the senescent state is dependent on the ECM. Our data also suggest that, despite their proliferative arrest, senescent cells maintain an intrinsic and latent capacity to proliferate, and that exposure to ECM derived from young cells stimulates this latent mitogenic potential. This finding indicates a need to reevaluate the conventional idea that mitogenic potential of senescent cells is irreversibly lost.

To the best of our ability our idea was to detect Y-ECM successfully restored senescent cells to a more youthful state that was indistinguishable from that of normal young cells. Multiple phenotypes of the senescent cells were partially or fully reversed by Y-ECM, including SA-β-gal expression, intracellular ROS

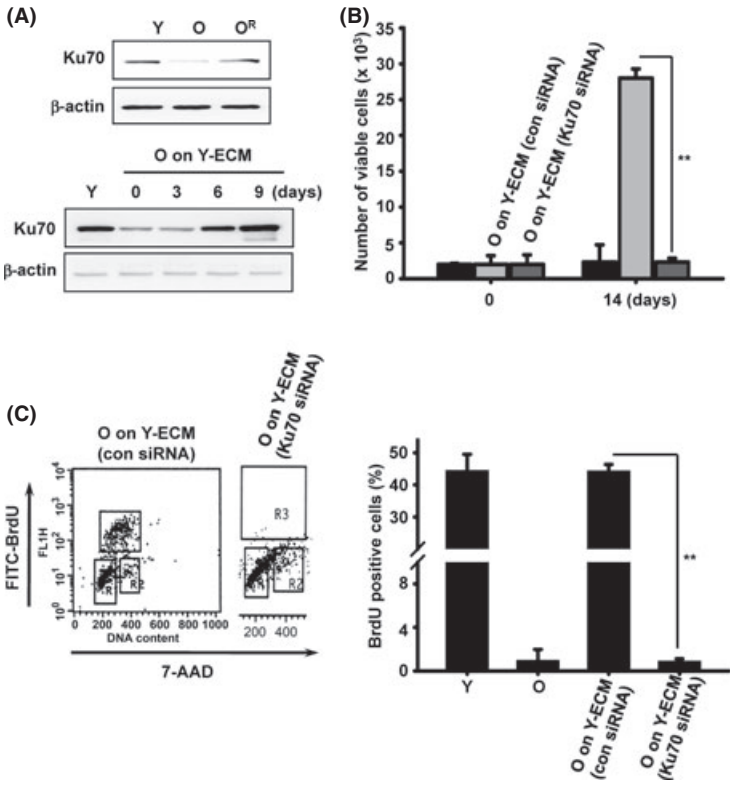

Fig. 4 Ku is required for restoration of senescent cells (A) Analysis of Ku70 protein expression in young, senescent and restored senescent cells by Western blotting (first panel). Analysis of Ku70 protein expression during the restoration process (second panel). Senescent cells were cultured on extracellular matrix from young cells treated with control and Ku70 siRNA. Analysis of the number of viable cells (B) and BrdU incorporation rate (C) after 14 days. The results shown are representative of three independent experiments; the histograms indicate the mean and the error bars indicate the standard deviation of the mean. A value of $P < 0.01$ was considered statistically significant. A double asterisk (**) denotes $P < 0.01$ in a Student's *t* test.

levels, F-actin staining, mitochondrial membrane potential, DNA damage foci, telomere length, and expression of multiple senescence-related genes such as p53, p16, p21, and caveolin-1 (Figs 2 and 3). While we cannot rule out the possibility that restored cells differ in some undetected way from normal young cells, it is clear that they resemble young cells in many important ways (Figs S1 and S2). Notably, the restoration of youthfulness by Y-ECM did not confer immortality, as restored cells went through a growth period followed by apparently normal senescence (Fig. 2F–H). It will be of interest in future studies to determine whether these restored cells grown to senescence can be restored again by new Y-ECM and, if so, what limits (if any) exist for sequential restoration of senescent fibroblasts.

Our observations naturally beg the question as to what molecular mechanisms might account for restoration of senescent fibroblasts by Y-ECM. Within the cell, it seems likely that telomere elongation plays an important role and, indeed, telomeres are elongated in the restored cells (Fig. 3C). Although we cannot rule out the possibility that telomerase is transiently induced during the restoration process, we were unable to detect telomerase expression in restored cells, suggesting that telomere restoration may occur by a telomerase-independent mechanism (Fig. 3D).

Ku proteins are important for maintaining proper telomere structure and function, and Ku activity is regulated by the SIRT1 deacetylase (Fig. 5) (Gasser, 2000; Tham & Zakian, 2000; Indiviglio & Bertuch, 2009). It is therefore of interest that Ku and SIRT1 expression decrease during senescence and is reestablished during restoration (Figs 4A and 5A). The observation that senescent cells are not restored by Y-ECM from young cells treated with Ku70 or SIRT1 siRNA demonstrates that both Ku and SIRT1 are essential components determining how young cells influence their microenvironment. The fact that the SIRT1 inhibitor EX-527 blocks restoration indicates that SIRT1 catalytic activity is crucial, and suggests the model that SIRT1 deacetylation of Ku allows young cells to produce Y-ECM with the capacity to restore old, senescent cells. Of course, additional SIRT1 targets may also be involved in the restoration process, and it will be important to furthermore define the role of SIRT1 in senescence and restoration of senescent cells.

Our findings also bear similarity to *in vivo* studies of adult muscle stem cells showing that the reduced proliferative capacity with age is noncell autonomous and restorable in parabiosis studies where they are exposed to blood supply from young mice (Conboy *et al.*, 2005). We propose the existence of a generalized pathway by which aged cells in the adult organism interpret their surroundings and make decisions about whether to proliferate. If so, it may be possible to design therapeutic regimens that manipulate these pathways in an effort to restore youthful behavior in aged adult stem cell populations.

Conclusion

The data described here counter traditional views on the reversibility of cell senescence, demonstrating that it is possible to restore 'irreversibly' senescent cells to an apparently normal,

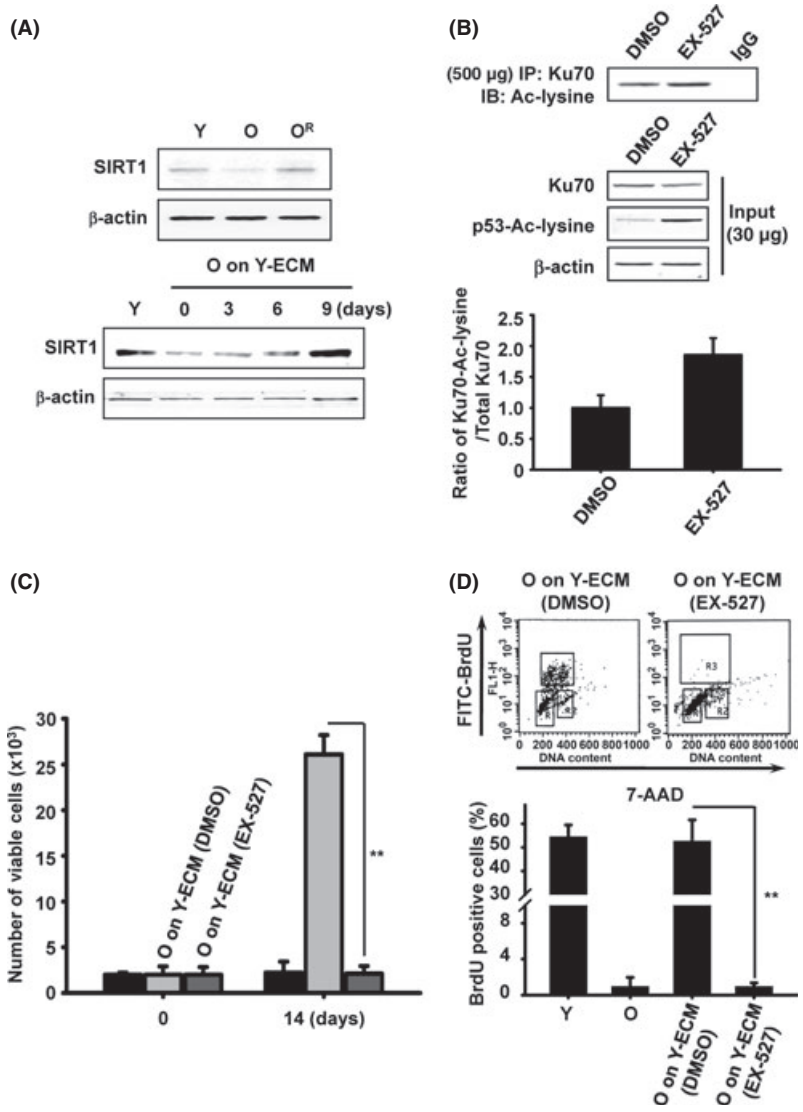

Fig. 5 SIRT1 activity is required for restoration (A) Analysis of SIRT1 protein expression in young, senescent, and restored senescent cells by Western blotting (first panel). During the restoration process, SIRT1 protein expression was analyzed by Western blotting (second panel). (B) Young cells were treated with 400 nM Trichostatin A in the presence or absence of EX-527. Cell lysates were immunoprecipitated with anti-Ku70. Ku70 acetylation was determined by Western blotting with anti-acetyl-lysine antibody (first panel). Effect of EX-527 on Ku70 and p53-acetylation was determined by Western blot (second panel). Histogram indicates acetylation of Ku70 after EX-527 treatment in young cells. Senescent cells were cultured on extracellular matrix derived from young cells treated with control (DMSO) and 1 μM EX-527. Analysis of the number of viable cells (C) and BrdU incorporation rate (D) after 14 days. The results shown are representative of three independent experiments; histograms indicate the mean and error bars indicate the standard deviation of the mean. A value of $P < 0.01$ was considered statistically significant. A double asterisk (**) denotes $P < 0.01$ in a Student's *t* test.

youthful state by a simple correction of environmental cues. Although this effect has, thus far, only been observed *in vitro*, we suggest the possibility that *in vivo* cellular senescence could be similarly altered by appropriately modulating the microenvironment of target cells. If correct, this possibility could have important implications for the treatment of age-related diseases.

Experimental procedures

Reagents and instruments

The sources of reagents used are as follows: The antibody to caveolin-1 (sc894), phospho-Erk (sc7383), Erk-1/2 (sc94), p53 (sc126), p16 (sc759), p21 (sc756), and SIRT1 (sc15404) were from Santa Cruz Biotechnology, Inc. (Santa Cruz, CA, USA). Anti-mouse antibody Ku70 (ab3107) was from Abcam (Cambridge, MA, USA). Polyclonal anti-acetyl-Lysine (06-933) antibody was from Millipore (Billerica, MA, USA). Trichostatin A (9950) was from Cell Signaling (Danvers, MA, USA). The Alexa fluor 568 phalloidin, CM-H_2DCF-DA was from Molecular Probes (Carlsbad, CA, USA). Comet assay instruction (4250-050-K) was from Trevigen (Gaithersburg, MD, USA). FITC BrdU Flow kit (559619) was from BD (San Jose, CA, USA) (Pearson *et al.*, 2000). EX-527 was purchased from Tocris (Avron BS110QL, UK).

Cell culture and ECM preparation

Neonatal young fibroblasts were isolated from a neonate, as descried (Boyce & Ham, 1983). Young human diploid fibroblasts (HDFs) were isolated from foreskin of a 6-year-old boy. Briefly, cells were cultured in a 100 mm Φ dish at 37°C, 5% CO_2 in Dulbecco's modified Eagle's medium supplemented with 10% fetal bovine serum, 100 units mL^{-1} penicillin, 100 μg mL^{-1} streptomycin. Cellular senescence was confirmed by determining the

percentage of cells capable of DNA synthesis over a 3 day interval ([^{3}H] thymidine incorporation) and SA-β-gal activity assay. Extracellular matrix was prepared by culturing HDFs in DMEM with serum for 3 days. The medium was aspirated from the HDFs and the cells were washed with PBS, followed by washing with EDTA or Trypsin-EDTA (Invitrogen-15400054, Trypsin, 0.5% (10×) with EDTA 4Na) in PBS. The cells were incubated at 37°C for 5 min, and then the solubilized cells were aspirated off and replaced in cold PBS. Dishes (BD Falcon™-353003, 100-mm Φ cell culture dish, tissue-culture-treated polystyrene) containing ECM were kept at 4°C for longer than 1 day to detect any remaining cells and then cells were seeded on the ECM.

Measurement of mitochondrial membrane potential ($\triangle\Psi_m$)

To determine the effect of ECM on ($\triangle\Psi_m$), 0.3 ug mL^{-1} JC-1 (5,5′,6,6′-tetrachloro-1,1′,3,3′-tetraethylbenzimidalohylcarbocyanineiodidie; Invitrogen) was added to young, senescent, and restored cells. After 30 min at 37°C, cells were washed with PBS, trypsinized and collected in 1 mL PBS, and applied Fluorescence Activated Cell Sorting (FACS). The fluorescence at 585 nm (FL2) and 525 nm (FL1) was measured for the JC-1 treated cells as well as the mock-treated cells. To correct for autofluorescence, the FL2 and FL1 values from the JC-1-treated cells were subtracted with those from the mock treated cells. $\triangle\Psi_m$ was determined by dividing the corrected FL2 valued FL2 value by the corrected FL1 value (Kang & Hwang, 2009).

Telomere-dysfunction-induced foci assay

Cells were seeded on glass coverslips and allowed to recover for 48 h. Cells were fixed for 15 min at room temperature with 4% paraformaldehyde buffered solution, followed by permeabilization with 0.5% Triton X-100 for 10 min. Cell preparations were blocked for 1 h at room temperature in 5% bovine serum albumin. Cells were incubated with anti-gamma-H2AX (abcam-ab11174) for overnight at 4°C. Appropriate fluorescence-conjugated secondary antibodies (Invitrogen-A11008) were applied for 1 h at room temperature. After this slides were placed in 4% paraformaldehyde for 15 min for cross-fixing to preserve antibodies. The next step involved hybridization with telomeric peptide nucleic acid (PNA-Panagene-F1005-10) labeled probe and staining was analyzed using a fluorescence microscope.

Telomerase activity and telomere length assay

Telomerase activity was measured using the TRAPeze® XL Telomerase Detection kit (Chmicon-S7707; Billerica, MA, USA) and RT-PCR (hTERT gene expression). Total RNA (1 μg) was reverse transcript in 2000 U of M-MLV RT (invitrogen-18064-022), 0.2 μg Oligo (dT) primer and 0.5 μg deoxynucleotides. The reaction was performed for 10 min at 65°C and for 60 min at 42°C. After heat inactivation of reverse transcriptase at 70°C for 10 min, 2 μL of reverse transcriptase reaction and 48 μL of PCR reaction mixture [final concentration 2 mM $MgCl_2$, 1 U of Taq polymerase and hTERT primer (forward: 5′-AGA GTG TCT GGA GCA AGT TGC-3′ reverse: 5′-CGT AGT CCA TGT TCA CAA TCG), Quick PCR premix was from Genemed Inc. (South San Francisco, CA, USA).] were mixed and PCR-amplified. The reaction was performed for 35 cycles at 94°C for 1 min, 65°C for 1 min and 72°C for 2 min. For telomere-length analysis, 10 μg of genomic DNA were digested with *Hin*fI and *Rsa*I and analyzed by southern blotting (Roche-12-209-136-001; Indianapolis, IN, USA) and Real-time quantitative PCR (Gil & Coetzer, 2004). We harvested young cells (PD 20-30), senescent cells, (over PD 68) and restored senescent cells (PD 2) for telomere analysis.

Colony formation assay in soft agar

For making soft agar and hard agars, 2.2% agar stock with PBS was prepared. A quantity of 0.75 mL agar stock was mixed with 1.75 mL DMEM containing 10% fetal bovine serum, 100 units mL^{-1} penicillin, 100 μg mL^{-1} streptomycin for hard agar. They were plated on 60 mm Ø culture dishes. After drying, 1×10^4 cells were plated on the hard agar with 0.5 mL agar stock and 2 mL DMEM. The dishes were incubated at 37°C in 5% CO_2 and cells were counted under the microscope at 12 ± 2 days.

In vitro transfection of Ku70 siRNA

Double stranded siRNA targeting human Ku70 was synthesized by Dharmacon Research (Lafayette, CO, USA). A synthetic siRNA SMARTpool duplex corresponding to the Ku70 mRNA was used to inhibit Ku70 and Ku80 protein expression (Ku70-siGENOME SMARTpool M-005084-01-0005 and KU80-siGENOME SMARTpool M-010491-00-0005). SiRNA SMARTpool duplexes in a 1× siRNA buffer (diluted from 5× siRNA buffer – Dharmacon product B-002000-UB-100) were transfected with cells. Transfection with siRNA was performed using planted Lipofectamine RNAi MAX (Invitrogen-13778-150) in Opti-MEM® I Medium without serum and incubated at 37°C in CO_2 incubator.

Immunoprecipitaion (determination of acetylated Ku70 levels)

To determine the effects of deacetylase inhibitors on Ku70 acetylaion levels, cells were treated with 400 nM Trichostatin A (TSA) and 1 uM EX-527 in young cells. The cells were lysed in a lysis buffer (20 mM Tris-HCl (pH 7.5), 150 mM NaCl, 1 mM EDTA, 1 mM Ethylene glycol tetraacetic acid (EGTA), 1% Triton X-100, 2.5 mM sodium phosphate, 1 mM β-glycerolphosphate, 1 mM phenylmethylsulphonyl fluoride, 1 mM sodium orthovanadate, 100 mM sodium fluoride, complete Protease Inhibitor Cocktail (Rhoche-11836153001), 1 μg mL^{-1} Leupeptin and supplemented with 10 uM TSA (Cell Signaling-9950) and 5 mM nicotinamide (Calbiochem-48-1907; Gibbstown, NJ, USA) to prevent

deacetylation after cell lysis. Immunoprecipitation of Ku70 was performed with Ku70 monoclonal antibody overnight at 4°C, followed by incubation with PureProteome™ Protin A-beads (Millpore-LSKMAGA10). Beads were washed extensively with lysis buffer. Cell lysates or immunoprecipitates were resolved on 10% SDS gels.

Statistical analysis

Values are presented as means ± SEM (Fig. 2E, $n = 3$; Fig. 3A, $n = 70$; Fig. 3B, $n = 50$; Fig. 4D, $n = 3$; Fig. 5D, $n = 3$ and Fig. S3A, $n = 20$ samples per group) Significance between means was assessed by analysis of variance (ANOVA), followed by the Fisher's test or the Wilcoxon Signed Ranks test for multiple comparisons. $P < 0.01$ was considered significant.

Acknowledgments

This work is supported by grants from the Korea Research Foundation for Health Science and the National Research Foundation (NRF) through the Center for Ageing and Apoptosis Research at Seoul National University (RII-2002-097-05001-0, RII-2002-097-00001-0 and RII-2002-097-08004-0), Grant 2010-0029150 and the SNU BK21 program from the Ministry of Education, Science and Technology. MK is an Ellison Medical Foundation New Scholar in Aging. We deeply appreciate Professor Hai Won Chung of Department of Public Health, Seoul National University, for his generous suggestion and provision of materials on Comet assay. We are grateful to Professor Brian K. Kennedy of Buck Institute for Age Research for discussion of this project and for editing the manuscript.

Author contributions

Study conceived and planned by H.R.C., K.A.C., Y.S., M.K. and S.C.P.; experimental work by H.R.C., K.A.C. and H.T.K.; data analysis by H.R.C, K.A.C. I.K.C and S.C.P; finger printing analysis and analyzed the data by J.B.L.; manuscript composition by H.R.C., K.A.C., Y.S., M.K. and S.C.P.; all authors discussed the results and commented on the manuscript and S.C.P. supervised the entire project.

References

d'Adda di Fagagna F (2008) Living on a break: cellular senescence as a DNA-damage response. *Nat. Rev. Cancer* **8**, 512–522.

d'Adda di Fagagna F, Reaper PM, Clay-Farrace L, Fiegler H, Carr P, Von Zglinicki T, Savetzki G, Carter NP, Jackson SP (2003) A DNA damage checkpoint response in telomere-initiated senescence. *Nature* **426**, 194–198.

Allsopp RC, Vaziri H, Patterson C, Goldstein S, Younglai EV, Futcher AB, Greider CW, Harley CB (1992) Telomere length predicts replicative capacity of human fibroblasts. *Proc. Natl. Acad. Sci. U S A* **89**, 10114–10118.

Astrom SU, Okamura SM, Rine J (1999) Yeast cell-type regulation of DNA repair. *Nature* **397**, 310.

Blackburn EH (1990) Telomeres and their synthesis. *Science* **249**, 489–490.

Boyce ST, Ham RG (1983) Calcium-regulated differentiation of normal human epidermal keratinocytes in chemically defined clonal culture and serum-free serial culture. *J. Invest. Dermatol.* **81**(1 Suppl), 33s–40s.

Campisi J, d'Adda di Fagagna F (2007) Cellular senescence: when bad things happen to good cells. *Nat. Rev. Mol. Cell Biol.* **8**, 729–740.

Canela A, Vera E, Klatt P, Blasco MA (2007) High-throughput telomere length quantification by FISH and its application to human population studies. *Proc. Natl. Acad. Sci. U S A* **104**, 5300–5305.

Cawthon RM, Smith KR, O' Brien E, Sivatchenko A, Kerber RA (2003) Association between telomere length in blood and mortality in people aged 60 years or older. *Lancet* **361**, 393–395.

Cohen HY, Miller C, Bitterman KJ, Wall NR, Hekking B, Kessler B, Howitz KT, Gorospe M, de Cabo R, Sinclair DA (2004) Calorie restriction promotes mammalian cell survival by inducing the SIRT1 deacetylase. *Science* **305**, 390–392.

Conboy IM, Conboy MJ, Wagers AJ, Givma ER, Weissman IL, Rando TA (2005) Rejuvenation of aged progenitor cells by exposure to a young systemic environment. *Nature* **433**, 760–764.

Critchlow SE, Jackson SP (1998) DNA end-joining: from yeast to man. *Trends Biochem. Sci.* **23**, 394–398.

Deng Y, Chan SS, Chang S (2008) Telomere dysfunction and tumour suppression: the senescence connection. *Nat. Rev. Cancer* **8**, 450–458.

Dimri GP, Lee X, Basile G, Acosta M, Scott G, Roskelley C, Medrando EE, Linskens M, Rubelj I, Pereira-Smith O (1995) A biomarker that identifies senescent human cells in culture and in aging skin in vivo. *Proc. Natl. Acad. Sci. U S A* **92**, 9363–9367.

Finkel T, Deng CX, Mostoslavsky R (2009) Recent progress in the biology and physiology of sirtuins. *Nature* **460**, 587–591.

Fisher TS, Zakian VA (2005) Ku: a multifunctional protein involved in telomere maintenance. *DNA Repair (Amst.)* **4**, 1215–1226.

Gasser SM (2000) A sense of the end. *Science* **288**, 1377–1379.

Gil ME, Coetzer TL (2004) Real-time quantitative PCR of telomere length. *Mol. Biotechnol.* **27**, 169–172.

Gorbunova V, Seluanov A (2009) Coevolution of telomerase activity and body mass in mammals: from mice to beavers. *Mech. Ageing Dev.* **130**, 3–9.

Haber JE (1999) Sir-Ku-itous routes to make ends meet. *Cell* **97**, 829–832.

Harley CB, Futcher AB, Greider CW (1990) Telomeres shorten during ageing of human fibroblasts. *Nature* **345**, 458–460.

Harman D (1956) Aging: a theory based on free radical and radiation chemistry. *J. Gerontol.* **11**, 298–300.

Hastie ND, Dempster M, Dunlop MG, Thompson AM, Green DK, Allshire RC (1990) Telomere reduction in human colorectal carcinoma and with ageing. *Nature* **346**, 866–868.

Hasty P (2001) The impact energy metabolism and genome maintenance have on longevity and senescence: lessons from yeast to mammals. *Mech. Ageing Dev.* **122**, 1651–1662.

Henson JD, Neumann AA, Yeager TR, Reddel RR (2002) Alternative lengthening of telomeres in mammalian cells. *Oncogene* **21**, 598–610.

Herbig U, Ferreira M, Condel L, Carey D, Sedivy JM (2006) Cellular senescence in aging primates. *Science* **311**, 1257.

Hynes RO (2009) The extracellular matrix: not just pretty fibrils. *Science* **326**, 1216–1219.

Indiviglio SM, Bertuch AA (2009) Ku's essential role in keeping telomeres intact. *Proc. Natl. Acad. Sci. U S A* **106**, 12217–12218.

Jeong J, Juhn K, Lee H, Kim SH, Min BH, Lee KM, Cho MH, Park GH, Lee KH (2007) SIRT1 promotes DNA repair activity and deacetylation of Ku70. *Exp. Mol. Med.* **39**, 8–13.

Jeyapalan JC, Sedivy JM (2008) Cellular senescence and organismal aging. *Mech. Ageing Dev.* **129**, 467–474.

Kaeberlein M, McVey M, Guavente L (1999) The SIR2/3/4 complex and SIR2 alone promote longevity in Saccharomyces cerevisiae by two different mechanisms. *Genes Dev.* **13**, 2570–2580.

Kang HT, Hwang ES (2009) Nicotinamide enhances mitochondria quality through autophagy activation in human cells. *Aging Cell* **8**, 426–438.

Kennedy BK, Gotta M, Sinclair DA, Mills K, McNabb DS, Murthy M, Park SM, Laroche T, Gasser SM, Guavente L (1997) Redistribution of silencing proteins from telemeves to the nucleolus is associated with extension of life span in *S. cerevisiae*. *Cell* **89**, 381–391.

Krtolica A, Parrinello S, Lockett S, Desprez PY, Campisi J (2001) Senescent fibroblasts promote epithelial cell growth and tumorigenesis: a link between cancer and aging. *Proc. Natl. Acad. Sci. U S A* **98**, 12072–12077.

Lee SE, Paques F, Sylvan J, Haber JE (1999) Role of yeast SIR genes and mating type in directing DNA double-strand breaks to homologous and non-homologous repair paths. *Curr. Biol.* **9**, 767–770.

Linnane AW, Marzuki S, Ozawa J, Tanaka M (1989) Mitochondrial DNA mutations as an important contributor to ageing and degenerative diseases. *Lancet* **1**, 642–645.

Longo VD, Kennedy BK (2006) Sirtuins in aging and age-related disease. *Cell* **126**, 257–268.

Lund TC, Glass TJ, Tolav J, Blazar BR (2009) Expression of telomerase and telomere length are unaffected by either age or limb regeneration in Danio rerio. *PLoS ONE* **4**, e7688.

Muggleton-Harris AL, DeSimone DW (1980) Replicative potentials of various fusion products between WI-38 and SV40 transformed WI-38 cells and their components. *Somatic Cell Genet.* **6**, 689–698.

Oberdoerffer P, Michan S, McVay M, Mostoslavsky R, Vann J, Park SK, Hartlerode A, Stegmuller J, Hafner A, Loerch P, Wright SM, Mills KD, Bonni A, Yankner BA, Scully R, Prolla TA, Alt FW, Sinclair DA (2008) SIRT1 redistribution on chromatin promotes genomic stability but alters gene expression during aging. *Cell* **135**, 907–918.

Olive PL, Banath JP (2006) The comet assay: a method to measure DNA damage in individual cells. *Nat. Protoc.* **1**, 23–29.

Park WY, Park JS, Cho KA, Kim DI, Ko YG, Seo JS, Park SC (2000) Up-regulation of caveolin attenuates epidermal growth factor signaling in senescent cells. *J. Biol. Chem.* **275**, 20847–20852.

Pearson M, Carbone R, Sebastiani C, Cioce M, Fagioli M, Saito S, Higashimoto Y, Appella E, Minucci S, Pandolfi PP (2000) PML regulates p53 acetylation and premature senescence induced by oncogenic Ras. *Nature* **406**, 207–210.

Pereira-Smith OM, Smith JR (1981) Expression of SV40 T antigen in finite life-span hybrids of normal and SV40-transformed fibroblasts. *Somatic Cell Genet.* **7**, 411–421.

Ryu SJ, Oh YS, Park SC (2007) Failure of stress-induced downregulation of Bcl-2 contributes to apoptosis resistance in senescent human diploid fibroblasts. *Cell Death Differ.* **14**, 1020–1028.

Seluanov A, Danek J, Hause N, Govbunova V (2007) Changes in the level and distribution of Ku proteins during cellular senescence. *DNA Repair (Amst.)* **6**, 1740–1748.

Takai H, Smogorzewska A, de Lange T (2003) DNA damage foci at dysfunctional telomeres. *Curr. Biol.* **13**, 1549–1556.

Tham WH, Zakian VA (2000) Telomeric tethers. *Nature* **403**, 34–35.

Tsukamoto Y, Kato J, Ikeda H (1997) Silencing factors participate in DNA repair and recombination in Saccharomyces cerevisiae. *Nature* **388**, 900–903.

Verdun RE, Karlseder J (2007) Replication and protection of telomeres. *Nature* **447**, 924–931.

Vijg J, Maslov AY, Suh Y (2008) Aging: a sirtuin shake-up? *Cell* **135**, 797–798.

Wang J, Walsh K (1996) Resistance to apoptosis conferred by Cdk inhibitors during myocyte differentiation. *Science* **273**, 359–361.

Wang RH, Sengupta K, Li C, Kim HS, Cao L, Xiao C, Kim S, Xu X, Zheng Y, Chilton B, Jia R, Zheng ZM, Appella E, Wang XW, Ried T, Deng CX (2008) Impaired DNA damage response, genome instability, and tumorigenesis in SIRT1 mutant mice. *Cancer Cell* **14**, 312–323.

Wright WE, Shay JW (2000) Telomere dynamics in cancer progression and prevention: fundamental differences in human and mouse telomere biology. *Nat. Med.* **6**, 849–851.

Supporting Information

Additional supporting information may be found in the online version of this article:

Fig. S1 Time-lapse live cell analysis during restoration process.

Fig. S2 RFP tagged senescent cell analysis during restoration process.

Fig. S3 Restored senescent cells by Y-ECM from neonatal cells.

Fig. S4 Ku70-deficient young cells have defect in telomere length.

Fig. S5 Effect of Ku70-acetylation in young, senescent, and restored senescent cells.

As a service to our authors and readers, this journal provides supporting information supplied by the authors. Such materials are peer-reviewed and may be re-organized for online delivery, but are not copy-edited or typeset. Technical support issues arising from supporting information (other than missing files) should be addressed to the authors.